

Adsorption of Methylene Blue by *Imperata Cylindrica*: Reaction Optimization by Response Surface Methodology (RSM)

N. F. M. Salleh^{1*}, F. F. Asmori², N. M. Shukri¹, S. F. M. Hanafiah¹

¹School of Health Sciences, Universiti Sains Malaysia, Health Campus, 16150 Kubang Kerian, Kelantan, Malaysia.

²Faculty of Chemical and Natural Resources Engineering, Universiti Malaysia Pahang, 26300 Gambang, Pahang, Malaysia.

ABSTRACT – *Imperata Cylindrica* (IC) is a solid waste that is readily available throughout the year known as one of the most important weed in the world and frequently causes major disposal issues. As a result, using IC as a low-cost adsorbent is beneficial from both, economic and environmental standpoint to remove colors from wastewater of textile industry. This work studies the reaction optimization of methylene blue (MB) removal using IC by response surface methodology (RSM). The RSM experiments were designed with 4 independent variables (initial adsorbent dosage, initial pH, initial dye concentration, and initial temperature) and 1 response variable (percent removal of MB). According to the pareto figure, the initial pH demonstrated the greatest impact on the percent removal of MB. The RSM data predicted the optimum condition of MB removal up to 86.61% using IC, by utilizing adsorbent dosage of 1.458 g/L, at 42 °C, initial pH of 6.8 and MB concentration of 235 ppm. The characterization analysis revealed the physicochemical properties of IC in the adsorption process.

ARTICLE HISTORY

Received: 10 Oct. 2021

Revised: 27 Oct. 2021

Accepted: 1 Nov. 2021

KEYWORDS

Imperata Cylindrica
Methylene Blue
Optimization
Response Surface
Methodology

INTRODUCTION

The textile dyeing process is the most unfriendly industrial process for the environment, and it is one of the factors that contributes to the water pollution. This procedure entails the creation of coloured wastewater, which contains a large number of high-concentration, complex components, and unmanageable organic compounds, and it is critical to remove dyes as soon as possible [1]. Various conventional techniques are available for color removals from coloured wastewater, such as adsorption, ion exchange, coagulation, and membrane technology [2–4]. Among others, adsorption has emerged as one of the most useful and comparably low-cost method for the decolorization of coloured wastewater. Adsorption of aqueous effluents by activated carbon is a popular treatment technology that has been utilised for a number of separation and purification procedures in industrial operations. On the other hand, activated carbon is a costly material and its regeneration for reuse adds to the price [5].

In recent years, a variety of agricultural products and by-products have been studied to eliminate dye, including rubber-leaf powder, spent grain, residual biogas slurry, and rice husk owing to the advantages of small initial costs and investments [6–9]. *Imperata Cylindrica* (IC), cogongrass as perennial grasses is an agricultural waste which is abundantly available throughout the year [10]. Therefore, finding applications for this waste would be beneficial from both an environmental and economic standpoint.

The ability of the IC as the low-cost adsorbent was studied for the removal of oil, heavy metals, and methylene blue [11–13]. However, several details of the adsorption process cannot be observed due to the limitation of the classical method. Therefore, this study aims to examine the optimum conditions of the removal of MB from aqueous solution by IC using RSM. In addition, using RSM, the effects of variables, the relationship between variables and response, and the optimum conditions of variables were examined from a small number of experiments. Interestingly, this is the first study conducted using FCCD, whereas previous researchers only focused on the factorial design of RSM [14].

Chemicals

Methylene blue (MB, $C_{16}H_{18}N_3S$, 319.86 g/mol, 668 nm), sodium hydroxide (NaOH), and hydrochloric acid (HCl) were purchased from Merck (M) Sdn. Bhd. Malaysia. All chemicals used in this work were spectroscopic grade with ultra-high purify (99.9%).

Adsorbent (*Imperata Cylindrica*) Preparation

The IC was collected around Kg. Kayu Besar, Kota Bharu, Kelantan. It was chopped into 1-2 cm long pieces, soaked in water overnight to eliminate any contaminants adhering to the surface, and then oven-dried for 24 hours at 80 °C. The particles were crushed and sieved until they were uniformly 355-600 μ m in size. Finally, the powder was stored in a bottle as an adsorbent.

Characterization of *Imperata Cylindrica*

The functional groups in the IC powder were identified using Fourier Transform Infrared (FTIR) analysis in the 4000-400 cm^{-1} range. The morphological feature of the samples were identified using scanning electron microscopy (SEM) with a 15 kV accelerating voltage.

Adsorption Experiment

Adsorption experiment was conducted according to the operating parameters designed by RSM, as listed in Table 2. In brief, specific amount of IC powder was added in a 250 mL conical flask containing 200 mL of MB solution with specific concentration. The pH of MB solution was adjusted using HCl and NaOH. The adsorption process was conducted under constant stirring at a rate of 300 rpm at specific temperature until it reached equilibrium. The sample was then taken at the proper time and centrifuged for 15 minutes at 3500 rpm. A UV-vis spectrophotometer was used to quantify the residual MB concentration. All of the experiments were carried out in triplicates. The MB removal percentages were calculated using Equation (1).

$$\text{Percentage removal (\%)} = \frac{C_o - C_t}{C_t} \times 100 \quad (1)$$

Where C_o (mg/L) and C_t (mg/L) are the initial concentration and concentration at any time, respectively.

Experimental Design and Optimization

RSM analysis using a face-centered central composite design (FCCD) was conducted using design expert software. The ranges and coded levels of the variables are listed in Table 1. The total number of tests undertaken was 26, with 24 factorial points, 8 axial points, and 2 replicates at the centre points.

Table 1. Coded levels for independent variables.

Independent variables	Symbol	Coded levels		
		-1	0	1
Absorbent dosage (g/L)	X_1	0.3	1.125	2
Initial pH	X_2	2	5	8
Initial concentration (ppm)	X_3	50	225	400
Temperature ($^{\circ}\text{C}$)	X_4	30	40	50

EXPERIMENTAL DESIGN AND OPTIMIZATION

RSM analysis

Table 2 displays the experimental design and outcomes of the MB removal experiment using IC as low-cost adsorbent. The quadratic model for the percent removal of MB is described in Equation (2), which is based on the RSM analysis:

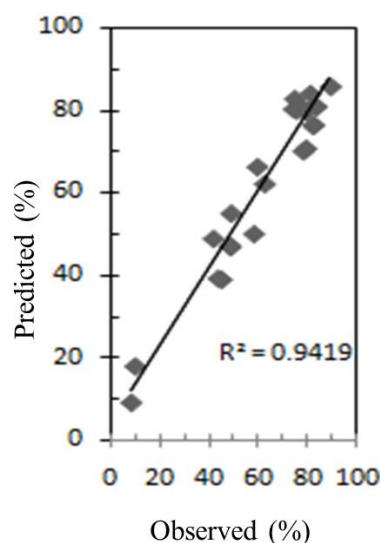
$$Y = 80.96 + 5.04X_1 + 18.63X_2 - 2.89X_3 - 0.04X_4 - 6.97X_1X_2 + 5.57X_1X_3 + 1.47X_1X_4 + 4.37X_2X_3 + 0.63X_2X_4 - 2.27X_3X_4 - 9.60X_1^2 - 15.48X_2^2 + 1.99X_3^2 - 1.02X_4^2 \quad (2)$$

where Y is a predicted percent removal of MB.

The percent removal of MB as seen in Figure 1 was compared to the projected values attained from Equation (2). The coefficient of determination (R^2) value for percent removal of MB is 0.9419, suggesting that the model accounts for 94.19% of the variability in the data. The empirical model is sufficient to elucidate the majority of the variability in essay reading, which should be at least 0.75 or more. Table 3 reveals that the F-value for percent removal of MB ($F_{0.05}=2.74$) is greater than the tabulated F-value ($F_{0.05}=2.74$). The model derived by Equation (2) can be concluded to give good predictions at a 5% level of significance.

Table 2. Experimental design and result of the response surface design.

No	Manipulated variables								Response
	X_1 (g)	Level	X_2 (pH)	Level	X_3 (ppm)	Level	X_4 (°C)	Level	Percentage removal of MB (%)
1	0.25	-1	2	-1	50	-1	30	-1	44.915
2	0.25	-1	2	-1	50	-1	50	1	43.615
3	0.25	-1	2	-1	400	1	30	-1	10.06
4	0.25	-1	2	-1	400	1	50	1	8.464
5	0.25	-1	8	1	50	-1	30	-1	79.412
6	0.25	-1	8	1	50	-1	50	1	74.576
7	0.25	-1	8	1	400	1	30	-1	82.335
8	0.25	-1	8	1	400	1	50	1	77.992
9	2	1	2	-1	50	-1	30	-1	41.667
10	2	1	2	-1	50	-1	50	1	48.837
11	2	1	2	-1	400	1	30	-1	58.046
12	2	1	2	-1	500	1	50	1	48.407
13	2	1	8	1	50	-1	30	-1	62.406
14	2	1	8	1	50	-1	50	1	79.152
15	2	1	8	1	400	1	30	-1	76.987
16	2	1	8	1	400	1	50	1	74.096
17	0.25	-1	5	0	225	0	40	0	59.388
18	2	1	5	0	225	0	40	0	81.823
19	1.125	0	2	-1	225	0	40	0	48.568
20	1.125	0	8	1	225	0	40	0	80.884
21	1.125	0	5	0	50	-1	40	0	89.086
22	1.125	0	5	0	400	1	40	0	75.303
23	1.125	0	5	0	225	0	30	-1	79.223
24	1.125	0	5	0	225	0	50	1	79.142
25	1.125	0	5	0	225	0	40	0	83.216
26	1.125	0	5	0	225	0	40	0	83.216

**Figure 1.** Parity plot for the observed and predicted values for reduction of MB

The analysis of variance (ANOVA) is shown in Table 3. The F-value for percent removal of MB is higher than the calculated F-value ($F_{0.05} = 2.74$). The big value of F suggests that the regression equation can explain the majority of the variation in the response. At a 5% level of significance, the model generated from Equation (4) can be concluded to give good predictions.

Table 3. ANOVA for percentage removal of MB model.

Sources	Sum of Squares (<i>SS</i>)	Degree of freedom (<i>d.f</i>)	Mean Square (<i>MS</i>)	<i>F</i> -value	$F_{0.05}$
Percentage removal of MB					
Regression (<i>SSR</i>)	9416.93	14	672.64	2.88	>2.74
Residual	2564.89	11	233.17		
Total (<i>SST</i>)	11981.83	25			

Figure 2 illustrates the Pareto chart and p-values of variables in Equation (4). The p-values are a technique for determining the effect of each coefficient. Each coefficient signifies higher relevance when the corresponding coefficient indicates fewer p-values or a larger magnitude t-value. As shown in Figure 2, the most significant effect on percent removal of MB is the linear term of effect of initial pH (X_2) with the smaller p-value (0.000001) and largest t-values (9.9365) as 95% significant level. For interaction term of adsorbent dosage and initial pH (X_1X_2), quadratic term of initial pH (X_2^2), the interaction term of adsorbent dosage and initial concentration (X_1X_3), and linear term of adsorbent dosage effect (X_1) could also be regarded as significant factors in affecting the percent removal of MB due to large t-values of -3.5076, -3.1151, 2.8022, and 2.6871, respectively.

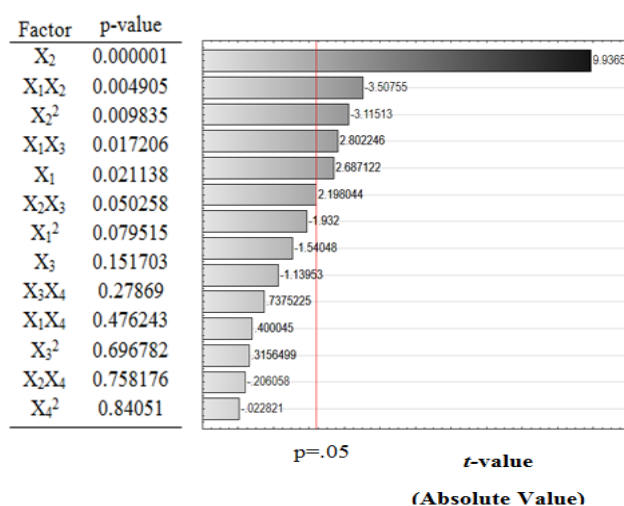


Figure 2. Pareto chart and p-value

The response surfaces are commonly used to assess the relationships between parameters and to forecast the outcome under particular circumstances. Six RSM 3-D plots between four parameters for the percent removal of MB model were generated and plotted as a function of two variables, with the others held constant at their mean values. Figure 3A shows a response surface plot of the percent removal of MB as a function of adsorbent dosage and initial pH. According to the examination of the response surface plot, initial pH value has a more significant influence on the response surface than adsorbent dosage. This can be explained by the Pareto chart (Figure 2), in which initial pH value has a higher t-value (9.9366) than adsorbent dosage (2.6871). The percent removal of MB rose as the initial pH value increased, peaking at pH 7 and then continuously increased as the adsorbent dosage increased until the maximum concentration of 1.4 g/L. The positive charge on the solution interface decreased as the pH climbed from pH 2 to 7, and the adsorbent surface appears to be negatively charged, rendering MB to rapidly adsorbed onto the surface of IC [15].

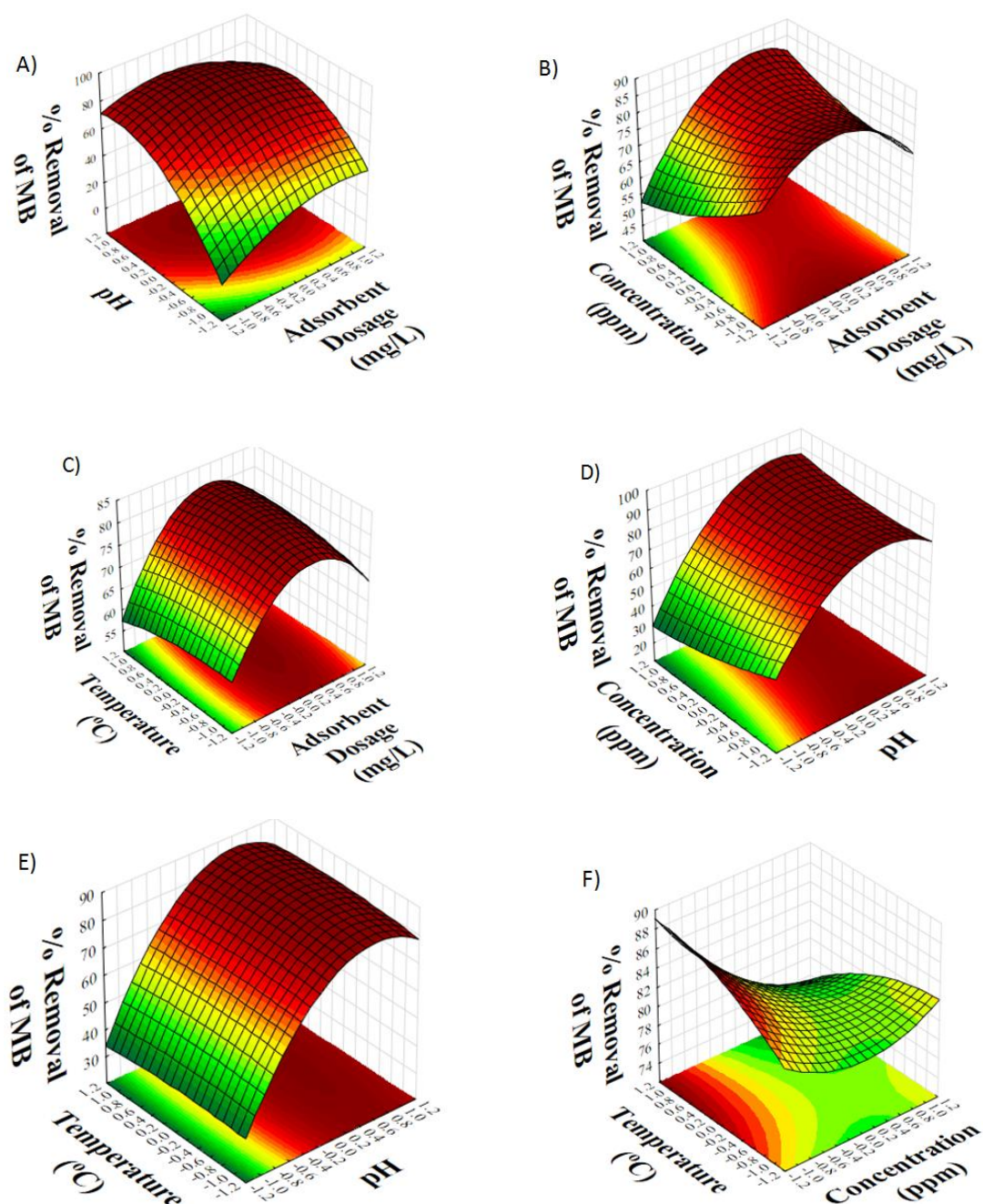


Figure 3. Response surface plot of combined (A) adsorbent dosage and pH, (B) initial concentration and adsorbent dosage, (C) adsorbent dosage and temperature, (D) concentration and pH, (E) temperature and pH and (F) temperature and concentration.

Figure 3B represents the effect of adsorbent dosage and concentration of MB on removal of MB. The increment of initial concentration of MB slightly affected the adsorption process, thus decreasing the percent removal of MB. As the initial MB concentration rises, the mass transfer driving force increases, resulting in less MB adsorption [16]. At low concentrations, the removal of MB only increases as the adsorbent dosage increases. However, for a higher removal of MB, a high concentration combined with a large adsorbent dose is required. This indicates that adsorption is strongly dependent on the dye concentration at the start. The initial number of dye molecules to accessible surface area ratio is low at lower concentrations. As a result, fractional adsorption is no longer dependent on the initial concentration. However, when the concentration increases, the number of accessible adsorption sites decreases, and as a result, the percentage of dye removed is proportional to the initial concentration. Figure 3C shows that the temperature of the MB solution has a minor impact on the removal of MB, whereas the adsorbent dosage has a considerable impact on the removal of MB. The adsorption of MB was marginally reduced when the surface coverage decreased. The surface area of the adsorbent is reduced as dye penetrates inside micro-pores or a new site is created at a higher temperature.

Figure 3D shows that the initial pH has a greater impact on the removal of MB than the initial MB concentration. This can be described by the bigger t-value of the initial pH value (9.9365) as compared to initial concentration (-1.13953). Figure 3E further illustrates that pH has a greater impact on the removal of MB as compared to temperature. This can be

elucidated by the bigger t-value of the initial pH value (9.9365) as compared to temperature (-2.0605). With an increase in the initial pH value, a progressive increase in the removal of MB was observed. However, after reaching the maximum, the percent removal of MB falls slightly when the initial pH value rises. The effect of temperature on the removal of MB was insignificant at constant pH. On the other hand, the relationship between temperature and MB concentration was not significant, as shown in Figure 3F. It is clear that these two variables, have little impact on MB adsorption. This finding is supported by the greater t-value of initial concentration (-1.13953) as compared to temperature (-2.0605) [17]. This observation is in agreement with the finding shown in Figure 3F, whereby the temperature has little effect on the adsorption of MB for the response surface plot of combined temperature and concentration.

In summary, all of the parameters appeared to have an impact on the percent removal of MB, but the initial pH appears to be the most important, in agreement with the greater t-value (9.9365). This is due to the fact that the pH affects not only the surface charge of the adsorbent in the solution, but also the degree of ionisation and dissociation of the functional groups on the active sites.

The optimum condition was forecasted from the response surface analysis, and the forecasted optimum percent removal of MB is 86.61%, at an adsorbent dosage of 1.458 g/L, temperature of 42 °C, initial pH of 6.8 and concentration of MB of 235 ppm. Validation of optimized result was conducted by comparing the observed value with the forecast value. The error (1.3%) was considered small within the 5% level of significance.

Characterization of adsorbent

The appearance and structure of the IC surface were studied using SEM before and after the 50-minute adsorption process, as illustrated in Figure 4. As shown in Figure 4a, IC has a rough surface with a heterogeneous porous and cavity structure. This suggests that MB dye could be trapped and absorbed into the surface of IC. However, the SEM image of IC after adsorption (Figure 4b) indicated that the caves, pores, and surfaces have been coated with MB.

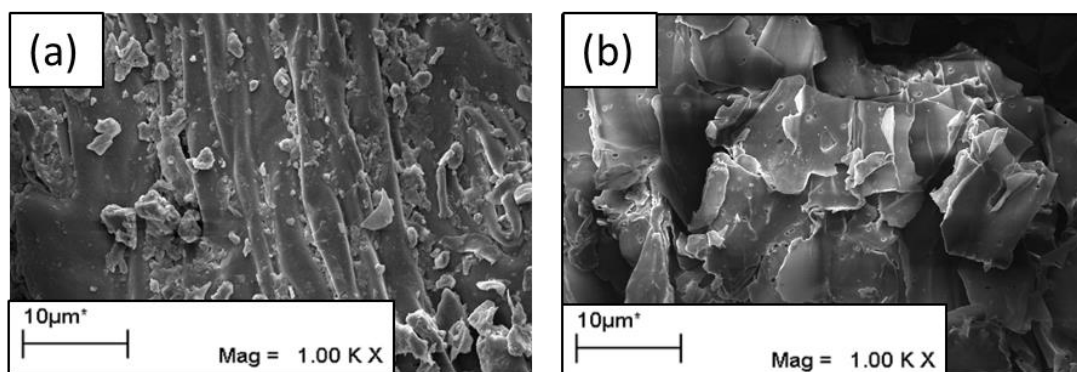


Figure 4. SEM micrograph of (a) IC before adsorption process (b) IC after 50 min of the adsorption process

The FTIR spectra of IC before and after the MB adsorption are shown in Figure 5. The broad peaks detected at 3434 and 3435 cm^{-1} could be assigned to O-H stretching vibration of hydroxyl functional group [18]. Meanwhile, the peaks at 2800-2852 cm^{-1} and 1602-1740 cm^{-1} were assigned to C-H stretching vibration and NH_2 deformation [19]. The intensities of the peaks become weaker after the adsorption process because the surface of the IC was occupied with the MB, and it slows down the adsorption process. Other peaks detected on IC before adsorptions were located at 1164 cm^{-1} assigned to C-N stretching vibration [20]. Nevertheless, these functional group disappeared after MB adsorption. The FTIR analysis indicated that IC has a lot of absorption peaks, which reflects the adsorbent's complex composition. The alterations in the spectrum after MB adsorption suggested the participation of the IC's functional groups in the MB adsorption process.

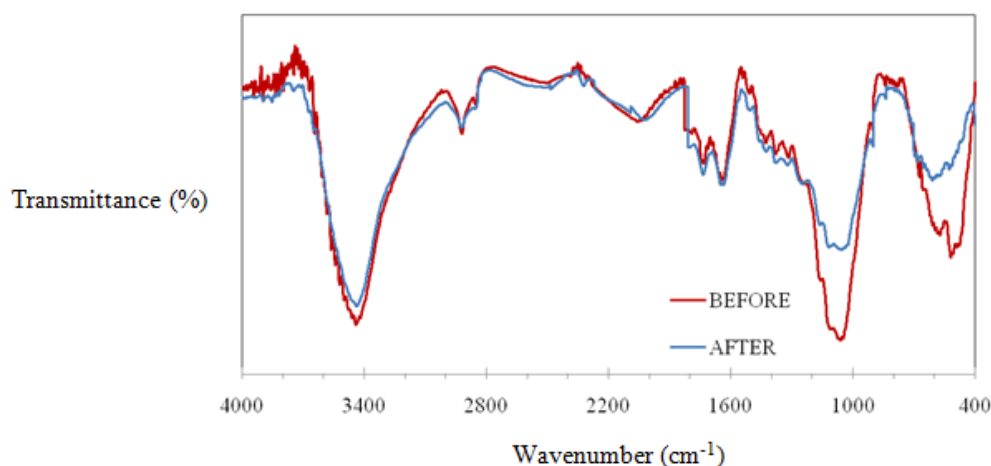


Figure 5. FTIR spectra of IC before and after MB adsorption

CONCLUSION

In summary, the IC as a low-cost adsorbent were successfully synthesized to remove colors from wastewater. This work also studies the reaction optimization of Methylene Blue (MB) removal using IC by RSM. The RSM experiments were designed with 4 independent variables (initial adsorbent dosage, initial pH, initial dye concentration, and initial temperature) and 1 response variable (percent removal of MB). According to the Pareto figure, the initial pH has the greatest impact on the percent removal of MB. The RSM data predicted the optimum condition of MB removal up to 86.61% using IC, obtained by utilizing adsorbent dosage of 1.458 g/L, at 42°C, with initial pH of 6.8 and MB concentration of 235 ppm. The characterization analysis confirmed the role of the IC's physicochemical properties in the adsorption process. The combined effects of independent variables (adsorbent dosage, pH, initial concentration, and temperature) on response (% MB removal) were investigated using RSM. The linear term of the initial pH was the greatest effect, according to the Pareto chart. The predicted value for the percent removal of MB at the optimum condition is 86.6%, respectively, with a small error of 1.3%. The optimum conditions for the removal of MB were observed at 1.458 g/L of IC, pH 6.8, 235 ppm of MB concentration, and 42 °C. As a conclusion, these findings are useful for designing adsorbents, as well as other materials for various applications.

ACKNOWLEDGMENT

We would like to thank the School of Health Sciences, Health Campus, Universiti Sains Malaysia for the technical assistance and supports in this work.

REFERENCES

- [1] R. P. Singh, P. K. Singh, R. Gupta, and R. L. Singh, "Treatment and Recycling of Wastewater from Textile Industry," pp. 225-266, 2019, DOI: 10.1007/978-981-13-1468-1_8
- [2] A. E. Al Prol, "Study of Environmental Concerns of Dyes and Recent Textile Effluents Treatment Technology: A Review," *Asian J. Fish. Aquat. Res.*, vol. 3, no. 2, pp. 1–18, 2019, doi: 10.9734/ajfar/2019/v3i230032.
- [3] E. M. Ijanu, M. A. Kamaruddin, and F. A. Norashiddin, "Coffee processing wastewater treatment: a critical review on current treatment technologies with a proposed alternative," *Appl. Water Sci.*, vol. 10, no. 1, pp. 1–11, 2020, doi: 10.1007/s13201-019-1091-9.
- [4] V. Katheresan, J. Kansedo, and S. Y. Lau, "Efficiency of various recent wastewater dye removal methods: A review," *J. Environ. Chem. Eng.*, vol. 6, no. 4, pp. 4676–4697, 2018, doi: 10.1016/j.jece.2018.06.060.
- [5] N. A. Bakar et al., "An insight review of lignocellulosic materials as activated carbon precursor for textile wastewater treatment," *Environ. Technol. Innov.*, vol. 22, p. 101445, 2021, doi: 10.1016/j.eti.2021.101445.
- [6] W. J. Yang et al., "Carbon quantum dots (CQDs) nanofiltration membranes towards efficient biogas slurry valorization," *Chem. Eng. J.*, vol. 385, no. October 2019, p. 123993, 2020, doi: 10.1016/j.cej.2019.123993.
- [7] S. Nag, A. Mondal, N. Bar, and S. K. Das, "Biosorption of chromium (VI) from aqueous solutions and ANN modelling," *Environ. Sci. Pollut. Res.*, vol. 24, no. 23, pp. 18817–18835, 2017, doi: 10.1007/s11356-017-9325-6.
- [8] Z. Jiang and D. Hu, "Molecular mechanism of anionic dyes adsorption on cationized rice husk cellulose from agricultural wastes," *J. Mol. Liq.*, vol. 276, pp. 105–114, 2019, doi: 10.1016/j.molliq.2018.11.153.
- [9] H. A. Chanzu, J. M. Onyari, and P. M. Shiundu, "Brewers' spent grain in adsorption of aqueous Congo Red and malachite Green dyes: Batch and continuous flow systems," *J. Hazard. Mater.*, vol. 380, no. March, p. 120897, 2019, doi: 10.1016/j.jhazmat.2019.120897.
- [10] N. Srinivasababu, *Understanding the durability of long sacred grass/Imperata cylindrica natural/hybrid FRP composites*. Elsevier Ltd, 2018.
- [11] L. Bulgariu et al., "The utilization of leaf-based adsorbents for dyes removal: A review," *J. Mol. Liq.*, vol. 276, pp. 728–747, 2019, doi: 10.1016/j.molliq.2018.12.001.
- [12] H. J. Hadi, K. M. M. Al-Zobai, and M. J. A. Alatabe, "Oil removal from produced water using Imperata cylindrica as low-cost adsorbent," *Curr. Appl. Sci. Technol.*, vol. 20, no. 3, pp. 494–511, 2020, doi: 10.14456/cast.2020.33.
- [13] M. Jaafar, A. Alatabe, and N. O. Kariem, "Using Imperata cylindrica as Natural Low-Cost Biosorbent for Rapid and Efficient Removal of Zinc (II) Ions from Aqueous Solutions," vol. 48, pp. 1226–1232, 2021.
- [14] C. X. H. Su, T. T. Teng, A. F. M. Alkarkhi, and L. W. Low, "Imperata cylindrica (cogongrass) as an adsorbent for methylene blue dye removal: Process optimization," *Water. Air. Soil Pollut.*, vol. 225, no. 5, 2014, doi: 10.1007/s11270-014-1941-x.
- [15] M. B. Ahmad, U. Soomro, M. Muqet, and Z. Ahmed, "Adsorption of Indigo Carmine dye onto the surface-modified adsorbent prepared from municipal waste and simulation using deep neural network," *J. Hazard. Mater.*, vol. 408, no. September 2020, p. 124433, 2021, doi: 10.1016/j.jhazmat.2020.124433.
- [16] A. B. Albadarin, M. N. Collins, M. Naushad, S. Shirazian, G. Walker, and C. Mangwandi, "Activated lignin-chitosan extruded blends for efficient adsorption of methylene blue," *Chem. Eng. J.*, vol. 307, pp. 264–272, 2017, doi: 10.1016/j.cej.2016.08.089.
- [17] R. Hasan and H. D. Setiabudi, "Removal of Pb(II) from aqueous solution using KCC-1: Optimization by response surface methodology (RSM)," *J. King Saud Univ. - Sci.*, vol. 31, no. 4, pp. 1182–1188, 2019, doi: 10.1016/j.jksus.2018.10.005.
- [18] R. Amiri, E. Khomehchi, and M. Ghaffarzadeh, "Experimental investigation of a novel multifunctional chemical solution on preventing asphaltene precipitation using two crude oil samples with different molecular properties," *J. Mol. Liq.*, vol. 309, p. 113121, 2020, doi: 10.1016/j.molliq.2020.113121.
- [19] S. K. Gaonkar and I. J. Furtado, "Valorization of low-cost agro-wastes residues for the maximum production of protease and lipase haloextremozymes by Haloferax lucentensis GUBF-2 MG076078," *Process Biochem.*, vol. 101, no. June 2020, pp. 72–88, 2021, doi: 10.1016/j.procbio.2020.10.019.
- [20] F. MaryAnjalin, N. Kanagathara, R. Gowri Shankar Rao, M. K. Marchewka, and S. Pugazhendhi, "Structural and spectroscopic aspects on anilinium hydrogen oxalate hemihydrate," *Mater. Today Proc.*, vol. 33, pp. 1049–1057, 2020, doi: 10.1016/j.matpr.2020.07.056.